Structural relaxation of the metastable Kasper phase of silicon

S. V. Demishev, D. G. Lunts, D. V. Nekhaev, N. E. Sluchanko, and N. A. Samarin

Institute of General Physics, Russian Academy of Sciences, 117942 Moscow, Russia

V. V. Brazhkin, A. G. Lyapin, and S. V. Popova

Institute of High-Pressure Physics, 142092 Troitsk, Moscow Region, Russia

N. N. Mel'nik

P. N. Lebedev Physics Institute, Russian Academy of Sciences, 117924 Moscow, Russia

(Submitted 23 November 1995)
Zh. Éksp. Teor. Fiz. **109**, 2150–2165 (June 1996)

The relaxation of the metastable Kasper phase of silicon SiIII, which is synthesized under high-pressure conditions, is investigated by step-by-step isothermal annealing. It is found on the basis of data from x-ray diffraction analysis and Raman scattering, as well as the electrophysical characteristics of the samples, that the lonsdaleite modification SiIV forms in this process and that the SiIII→SiIV phase transformation takes place in several stages, the appearance of a highly disordered quasiamorphous state of silicon being observed in the intermediate stage of the annealing. In the first stage (at annealing temperatures $T_{an} \leqslant 420$ K) the resistivity of the sample at $T=300$ K increases by more than two orders of magnitude as a consequence of a relaxation process in the Kasper phase of silicon. In the second stage of the transformation ($T_{an}=430$–450 K) the content of the Kasper phase decreases. For $T_{an} \sim 420$ K, a quasimetallic dependence of the conductivity is replaced by an activation dependence, and a metal–insulator transition occurs. For $T_{an} \geqslant 420$ K the activation energy for conduction increases smoothly until the resistivity changes are completed ($T_{an}=480$ K) and reaches saturation at a value of 0.35 eV. The total change in the electrical conductivity of the system in the region of the metal–insulator transition reaches 10^9 fold. In the Raman spectrum the intensity of the principal Kasper lines decreases to zero, and for $T_{an} \geqslant 470$ K, a broad, weakly structured feature forms at 430–520 cm^{-1}. The x-ray diffraction spectra of the sample in this stage of the transformation correspond to a mixture of microcrystalline and disordered phases: strongly broadened crystalline peaks of the lonsdaleite modification of silicon SiIV superposed on broad maxima are observed. In the third annealing stage ($T_{an}>490$ K) an appreciable quantity (20%) of the diamond-like phase SiI forms in the sample, and its volume fraction increases with the temperature. The heat of the SiIII→SiIV phase transition, equal to 8 kJ/mole, and the activation energy, 1.5 eV, are determined by scanning calorimetry. A simple crystal-geometric model is proposed, which qualitatively explains the appearance of the intermediate disordered state during the SiIII→SiIV phase transition. © *1996 American Institute of Physics.* [S1063-7761(96)01806-9]

1. INTRODUCTION

The metastable Kasper phase of silicon, SiIII, which belongs to the Ia^3 symmetry space group and has a coordination number $Z=4$ (Ref. 1), has been investigated in numerous studies by electron microscopy,[2] Raman scattering spectroscopy,[2–4] and x-ray diffraction analysis.[1,5] Its electrophysical parameters have also been measured.[6] In particular, it was established that when SiIII is heated to 470 K, it undergoes a transition to SiIV which has a lonsdaleite structure (space group D_{6h}^4, $Z=4$), rather than to the usual silicon phase SiI. Nevertheless, several features of this transition remain unclear. For example, the Raman scattering data show that several features in the spectra can be attributed to the formation of a-Si (Refs. 3 and 4). However, in Refs. 3 and 4 structural relaxation was induced by a laser pulse, and the process was not investigated in sufficient detail. In the only study[2] in which the quasi-isothermal step-by-step annealing of SiIII was carried out, only the time dependences of the resistivity of the samples were studied.

Several problems related to the structural relaxation of the metastable Kasper phase of silicon can be identified on the basis of the published data.

First, the Kasper phase is a semimetal,[2,6–8] in which metallic conductivity appears because of a small (~0.3 eV) overlap of the valence with conduction bands, while SiIV is a semiconductor with a band gap of ~0.7 eV (Ref. 9). For this reason, the character of the variation of the low-temperature electrophysical properties in the SiIII→SiIV transition is of interest.

Second, the details of the processes taking place during the SiIII→SiIV structural transformation have not yet been elucidated. Since most of the experiments were performed by laser annealing, the nature of the processes accompanying isothermal annealing is unclear.

Moreover, the energy of metastable SiIV is only slightly

higher than the energy of SiI, which is stable at $p = 1$ atm.[10] Therefore, the SiIV→SiI transformation should be expected when the temperature is increased further. The characteristics of this process and the possibility of its occurrence have likewise not been investigated.

Third, the study of the SiIII→SiIV structural transformation is also of interest in connection with the phenomenon of solid-phase amorphization. It has been established experimentally that strong disordering of the crystal structure of a sample and even its amorphization are often observed when a high-pressure metastable phase relaxes to normal conditions.[11,12] The physical mechanism of this phenomenon has not been thoroughly elucidated, but it can be presumed that the underlying process is the intensive formation of structural defects under the conditions of strong locally inhomogeneous stresses,[13] which are typical of various solid-phase amorphization processes.[13]

It was shown in Refs. 14 and 15 for bulk samples of amorphous gallium antimonide and a-GaSb that a "concentration degree of freedom," which allows local violations of the stoichiometric composition, can play a significant role in the appearance of solid-phase amorphization. In addition, in the case of a-GaSb the coordination numbers in the metastable and stable phases are different,[12,14,15]

Thus, there is considerable interest in an investigation of a situation in which the original substance is monatomic (there is no concentration degree of freedom) and the coordination numbers in the high- and low-pressure phases coincide.

The present work was devoted to an experimental investigation of these problems.

2. EXPERIMENTAL METHOD

Samples of single-crystal silicon with a diameter of 2–3 mm and a height of 1.5 mm were used to obtain the Kasper phase SiIII. The samples were heated to $T = 1300$ K by a nickel heating element at a constant pressure of 10 GPa in a "Toroid" chamber.[16] NaCl ampuls were used to prevent contamination of the sample. The temperature was monitored during the synthesis process by a Chromel–Alumel thermocouple.

The samples obtained were tested by x-ray diffraction analysis and Raman scattering spectroscopy. The Raman spectra were measured on a Jobin Yvon U-1000 spectrometer. The temperature dependences of the resistivity $\rho(T)$ and the thermopower $S(T)$, as well as the Hall coefficient at $T = 300$°C, were measured simultaneously. Five samples of SiIII having identical structural and electrophysical characteristics were selected for further investigation.

The samples of the Kasper phase were subjected to a series of isothermal anneals under an identical regime in the temperature range $T_{an} \approx 390$–480 K, which lasted 30–60 min and were separated by 10 K intervals. After each anneal the electrophysical characteristics and the Raman and x-ray diffraction spectra were measured. A detailed description of the step-by-step annealing technique was given in Ref. 15.

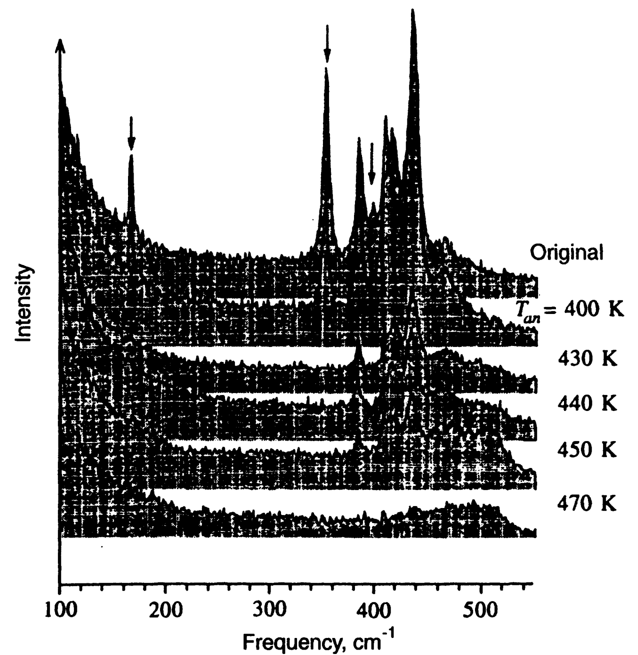

FIG. 1. Raman spectra for various stages of the annealing of the Kasper phase of silicon.

3. VARIATION OF THE STRUCTURE OF SiIII SAMPLES DURING ANNEALING

3.1. Raman spectra

It follows from an analysis of the symmetry of the crystal structure of SiIII that the vibrational spectrum contains nine different modes, of which only five are active in one-phonon Raman scattering.[2–4] The samples of the Kasper phase obtained according to the method described above are polycrystalline, locally stressed aggregates.[1–5] Therefore, the experimental Raman spectra display not only the five allowed lines, but also several additional maxima, which can be attributed to violation of the selection rules on the grain boundaries or in locally stressed regions.

Typical experimental Raman spectra of a sample of the Kasper phase of silicon are shown in Fig. 1. In the original state the Raman spectrum contains not only the five symmetry-allowed lines at 385, 409, 416, 434, and 468 cm^{-1} (Refs. 3 and 4), but also additional lines at 166, 352, and 397 cm^{-1} (the additional lines are marked by arrows in Fig. 1).

The evolution of the Raman spectra and the dependence of the intensity of the allowed and additional lines on the annealing temperature are presented in Figs. 1 and 2, respectively. It is seen from the Raman scattering data that the annealing of the SiIII samples takes place in two stages. In the first stage (390–420 K) the intensity of the additional lines decreases to zero, and the intensity of the allowed lines first increases somewhat and then begins to decrease at $T_{an} = 420$ K. Such behavior is consistent with the hypothesis that the "extra" lines appear as a result of a violation of the symmetry of the SiIII lattice caused by stresses on the grain boundaries and/or in the bulk of the sample. The resonance enhancement of Raman-forbidden modes may be an alterna-

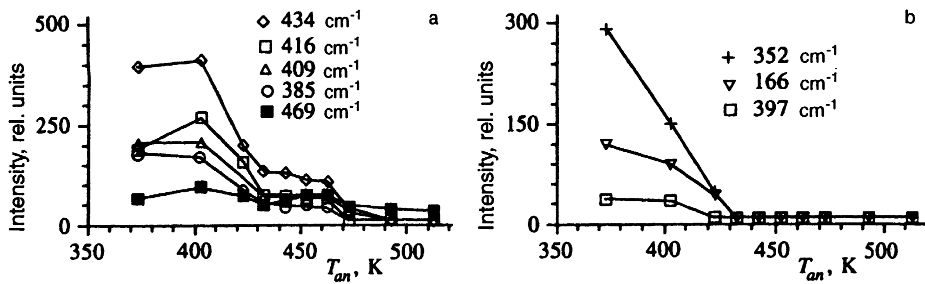

FIG. 2. Amplitude of allowed (a) and forbidden (b) lines in the Raman spectra as a function of the annealing temperature.

tive cause of the appearance of the additional modes. However, in that case a proportional decrease in the intensity of all the Kasper Raman maximum would be expected upon annealing, in contradiction to the experimental data (Figs. 1 and 2).

In the second stage of the transformation, i.e., in the range of annealing temperatures $T_{an}\approx 430-470$ K, there is a general decrease in the intensity of all the remaining allowed lines without variation of their widths (Fig. 1). At the same time, the intensity of the feature at 470–510 cm^{-1} increases markedly.

According to published data,[2-4,17-20] Raman modes for microcrystalline silicon in the form of μ-Si (510 cm^{-1}) and a-Si (480 cm^{-1}) and the allowed Kasper line at 470 cm^{-1} can be located in this region. The unequivocal identification of the contributions in this frequency range is complicated by the strong broadening and overlap of the lines.

When $T_{an}=470$ K is reached, all the lines of the original Kasper phase vanish completely, and the Raman spectra display a poorly structured, strongly broadened feature at 430–510 cm^{-1} (Fig. 1). Such behavior is naturally attributed to the strong disordering of the sample in this stage of the annealing. It is unlikely that such a broad feature can be caused by the microcrystallinity of the sample, since the broadening and the shift of the only Raman-active mode at 520 cm^{-1} for SiI do not exceed 30–40 cm^{-1} even in a finely dispersed crystal.[18-21]

When the annealing temperature is increased further to $T_{an}>470$ K, the relative amplitude of the line at 510-515 cm^{-1} increases (Fig. 3). At this point, the experimental spectrum can be satisfactorily approximated in the frequency range just indicated by the superposition of two lines: a broader line centered at 475–490 cm^{-1} and a narrower line located in the 510–515 cm^{-1} range (Fig. 3).

We note that such evolution of the Raman spectra with annealing is typical of the crystallization of amorphous silicon. In that case the broad line at approximately 480 cm^{-1} is assigned to a-Si, and the feature near 510 cm^{-1} is assigned to the microcrystals formed.

3.2. X-ray diffraction spectra

X-ray diffraction spectra for various annealing temperatures are presented in Figs. 4 and 5. The positions of the maxima in the spectrum of the original sample and the value of the cubic cell parameter $a=6.64\pm0.02$ Å are in good agreement with the literature data. The marked broadening attests to the microcrystalline structure of the sample appearing during the thermobaric treatment. Evaluation of the size of the coherent-scattering regions L from the Selyakov formula[22] shows that $L\approx 60-100$ Å in SiIII.

No significant changes occur in the x-ray scattering spectra in the range of annealing temperatures $T_{an}<420$ K (Fig. 4). In addition, no lines which could be associated with the presence of crystalline modifications of silicon differing from the Kasper phase are observed.

At $T_{an}=420$ K, the intensity of the 200 reflection ($2\theta\approx 12.53°$) begins to increase relative to the principal Kasper maxima. Such redistribution can be associated with

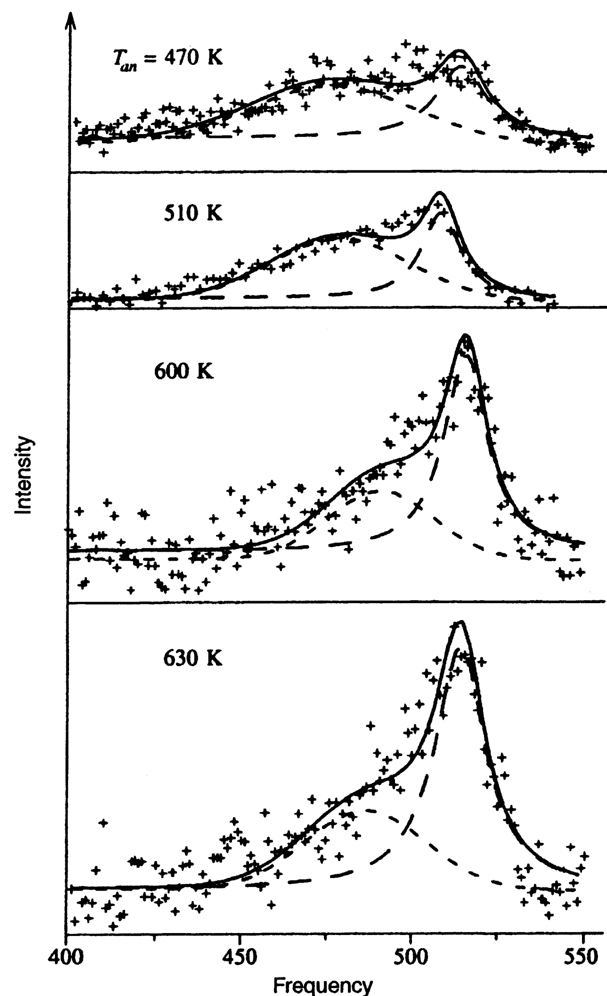

FIG. 3. Influence of annealing on the Raman spectra in the frequency range 400–550 cm^{-1} for $T_{an}\geqslant 470$ K.

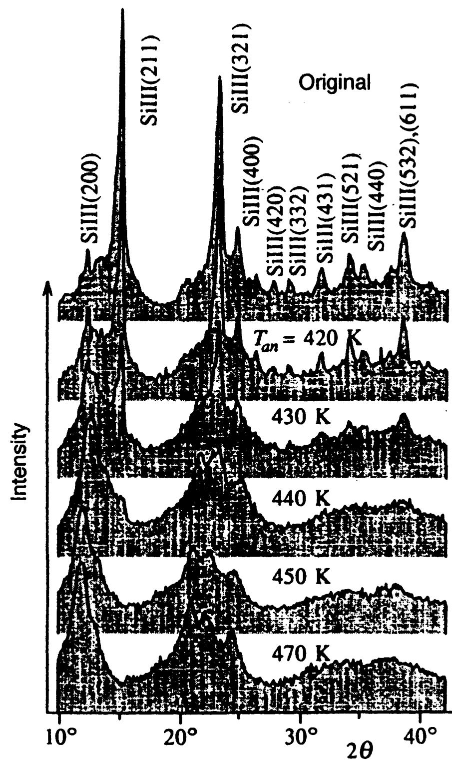

FIG. 4. X-ray diffraction spectra for various stages of the annealing of the Kasper phase of silicon for $T_{\mathrm{an}} \leqslant 470$ K.

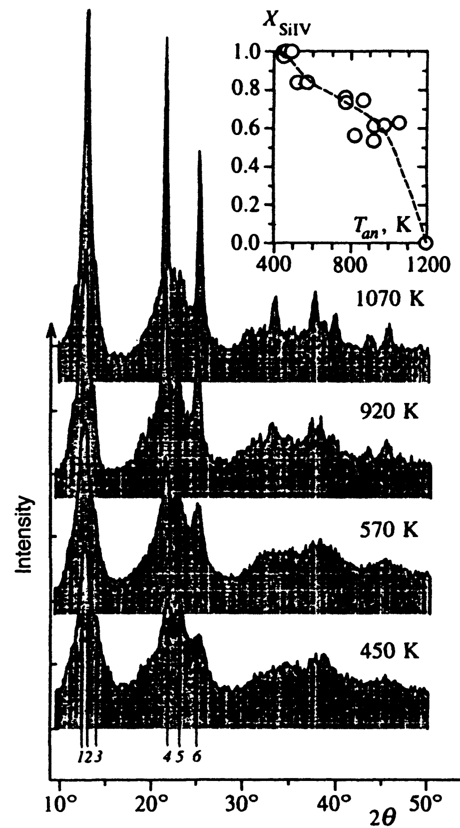

FIG. 5. X-ray diffraction spectra for various stages of the annealing of the Kasper phase of silicon for $T_{\mathrm{an}} \geqslant 450$ K. The arrows denote the following reflections: *1* – SiIV(100), *2* – SiIV(200) + SiI(111), *3* – SiIV(101), *4* – SiIV(110) + SiI(220), *5* – SiIV(301), *6* – SiIV(211) + SiI(311). In the inset X_{SiIV} is the fraction of SiIV.

the beginning of structural changes resulting from the relaxation of metastable SiIII. It is interesting that the strong 100 reflection ($2\theta \approx 12.35°$) of the lonsdaleite phase also appears in this region. Nevertheless, the total increase in intensity at $2\theta \approx 12°$ apparently cannot be caused by the appearance of inclusions of SiIV with a well-defined structure in the sample, since another peak would be expected to occur in that case at $2\theta \approx 21.5°$ for the intense 110 reflection of SiIV, which does not overlap with any Kasper peak. However, this feature cannot be identified against the background of the noise. This gives an upper estimate of 3–4% for the concentration of the lonsdaleite phase after annealing at 420 K.

For $T_{\mathrm{an}} = 430$ K the maxima corresponding to the lonsdaleite phase of silicon are appreciably stronger (Fig. 4), an "isolated" 110 reflection is displayed, and the relative intensity of the Kasper maxima drops.

Further annealing at 440 K results in the practically complete disappearance of the lines of the Kasper phase (Fig. 4). At this point narrower peaks corresponding to the lonsdaleite phase are observed superposed on broad maxima. Such a structure can appear in the spectrum for various reasons.

First, the possibility of the superposition of different crystalline lines from SiIII, SiI, and SiIV phases, some of which can be strongly broadened, should be taken into account. Second, the superposition of the narrow crystalline lines corresponding to SiIV and broad maxima can correspond to a mixture of amorphous (a-Si) and crystalline (SiIV) phases.

At an annealing temperature $T_{\mathrm{an}} > 440$ K the diffraction pattern corresponds completely to the tetrahedral lonsdaleite SiIV phase with the lattice constants $a = 3.634 \pm 0.006$ Å and $c = 6.33 \pm 0.01$ Å ($c/a = 1.65$) (Fig. 5), which agree with the published data[23] to within the experimental accuracy. Calculating the size of the coherent-scattering regions L for SiIV from the linewidth using the Selyakov formula and averaging over the different reflections, we can obtain the estimate $L \approx 20–30$ Å . This value is somewhat smaller than the size of a crystallite in the Kasper phase.

As the annealing temperature is increased, the x-ray diffraction spectra undergo characteristic evolution, which attests to the gradual conversion of the lonsdaleite SiIV phase with a hexagonal short-range order into diamond-like SiI (Fig. 5) and is fully completed when $T_{\mathrm{an}} \approx 1200$ K.

The quantitative ratio between the volume fractions of the diamond-like cubic phase and the hexagonal lonsdaleite phase as a function of the annealing temperature of the samples can be evaluated approximately from the calculated intensities of the crystalline reflections. The $(220)_c$ and $(311)_c$ reflections of the cubic diamond-like phase, as well as the $(110)_h$, $(103)_h$, and $(112)_h$ reflections of the lonsdaleite phase with hexagonal short-range order, which lie in the range of angles $2\theta = 18–26°$, were chosen for the calculation. The broad peak lying in this range of scattering angles on the experimental diffraction patterns can be represented as three Gaussian peaks superimposed on a diffuse contribution (up to $T_{\mathrm{an}} = 1000$ K), the ratio between the diffuse and co-

herent scatterings being weakly dependent on the annealing temperature. Also, the size of the coherent-scattering regions evaluated from the width of the peaks increases by 20–40% as T_{an} varies in the temperature range 600–1200 K.

The results of a quantitative evaluation of the intensity of the crystalline peaks and a comparison with the calculation showed how the concentration of the lonsdaleite SiIV phase varies with the annealing temperature (see the inset in Fig. 5). As a result, it was found that the content of the lonsdaleite phase x in the sample gradually decreases from $x=1$ ($T_{an}\leq 490$ K) to $x\approx 0.6$ ($T_{an}=1000$ K), after which active crystallization of the cubic diamond-like phase is observed.

Thus, an analysis of the x-ray diffraction and Raman spectra allows us to conclude that there are two stages in the phase transformation occurring when SiIII is annealed.

In the first stage ($T_{an}<430$–440 K) some redistribution of the intensities of the principal x-ray maxima and a drastic decrease in the intensities of the additional lines in the Raman spectra take place. No other crystalline modifications of silicon differing from the Kasper phase are observed in this stage, although the appearance of small amounts of SiIV cannot be ruled out. This process can apparently be associated with relaxation of the elastic stresses in the Kasper phase, which is manifested by the drop in the intensity of the additional maxima in the Raman spectra.

In the second stage ($T_{an}>440$ K) the rate of the phase transformation increases markedly. In this range of T_{an} the amplitudes of the x-ray and the principal Raman maxima corresponding to SiIII decrease sharply, and reflections corresponding to SiIV, which are superposed on broad maxima, appear in the x-ray diffraction spectra (Figs. 4 and 5). The Raman spectrum transforms into a broad structureless feature at 430–520 cm^{-1}, which is characteristic of a mixture of disordered and microcrystalline silicon.

4. METAL–INSULATOR TRANSITION UPON THE RELAXATION OF METASTABLE SiIII

The original samples of SiIII had p-type conductivity according to the signs of the Hall effect and the thermopower. The concentration $p\approx 6\times 10^{20}$ cm^{-3} and Hall mobility $\mu_H\approx 3$ $cm^2/V\cdot s$ were calculated from the values of the Hall coefficient and the resistivity at $T=300$ K.

The influence of annealing on the plots of the temperature dependence of the resistivity $\rho(T)$ for samples of the Kasper phase of silicon is shown in Fig. 6. It is seen that in the range of annealing temperatures $T_{an}\leq 440$ K the resistivity increases with T_{an}, but for $T_{an}\geq 460$ K the value of ρ ceases to depend on the annealing temperature, and the plots of $\rho(T)$ practically coincide.

It follows from the data in Fig. 6 that the annealing of SiIII samples induces a metal–insulator transition and that the absolute value of the resistivity at $T=150$ K increases by approximately 10^9 fold.

Let us now examine the metal–insulator transition in SiIII in greater detail. We first note that the plots of $\sigma(T)=[\rho(T)]^{-1}$ for $T_{an}\leq 410$ K can be transformed into a single dependence by means of scaling with the factor $\sigma_0/\sigma(T_i)$ (Fig. 7), where σ_0 is the conductivity of the

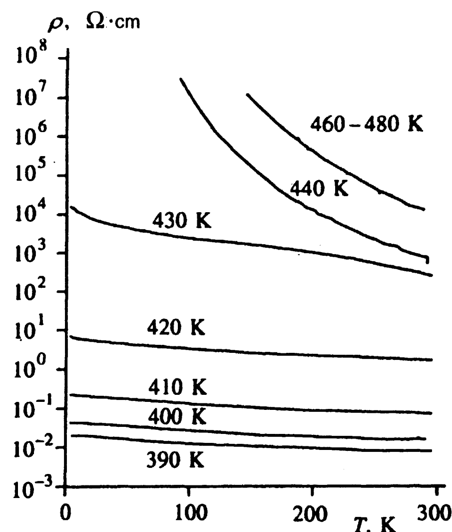

FIG. 6. Evolution of the temperature dependence of the resistivity during the annealing of the Kasper phase of silicon.

sample at $T=300$ K in the initial state and $\sigma(T_i)$ is the conductivity of the sample at $T=300$ K after annealing at $T_{an}=T_i$. The possibility of such a transformation means that percolation through the original low-resistance Kasper phase is maintained in this range of annealing temperatures as the geometry of the current paths varies with a resultant decrease in the total value of σ.

The plots of $\sigma(T)$ for $T_{an}=420$ K cannot be transformed into a single curve by similar scaling (Fig. 7). This qualitative difference is most clearly displayed at the low tempera-

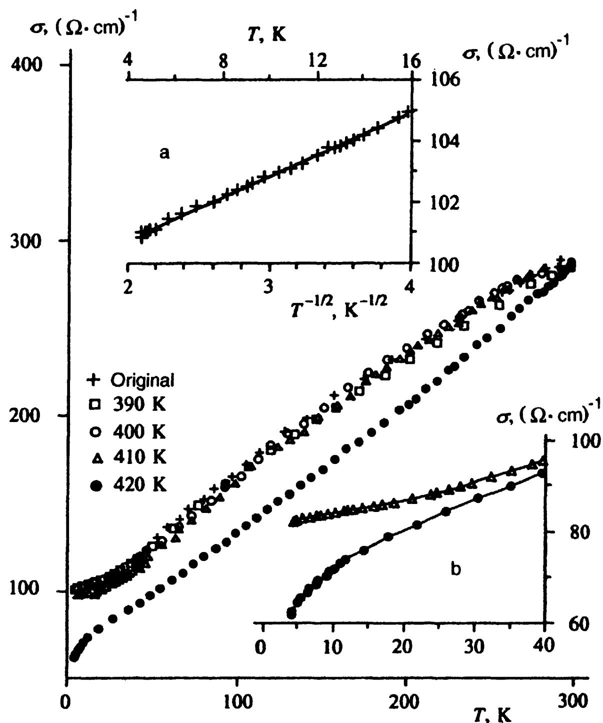

FIG. 7. Features of the conductivity at the metal–insulator transition induced by annealing SiIII.

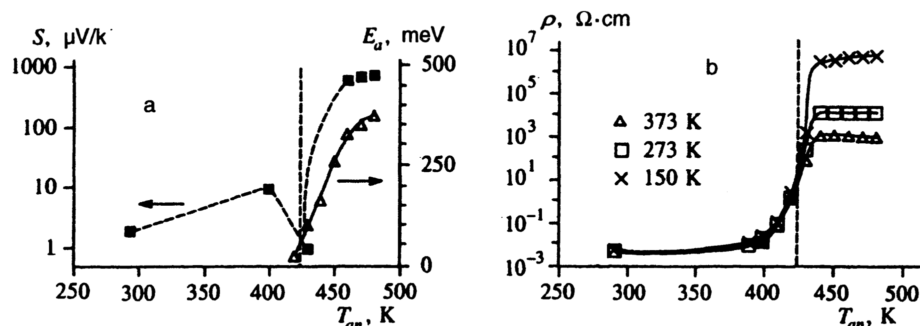

FIG. 8. Variation of the activation energy for conduction (a, △), the thermopower at $T=300$ K (a, ■), and the resistivity at various temperatures (b) in various annealing stages. The vertical dashed line corresponds to the point of the metal–insulator transition.

tures $T \leqslant 20$ K (see inset b in Fig. 7). In this temperature range the samples subjected to annealing at $T_{an} \leqslant 410$ K display an asymptotic behavior $\sigma \propto T^{1/2}$, which follows from the quantum corrections in the region of a metal–insulator transition[23] (see inset a in Fig. 7). At $T_{an}=20$ K, the segment corresponding to the low-temperature asymptotic form $\sigma \propto T^{1/2}$ vanishes. The power-law segment is replaced by a low-temperature conductivity "tail," and a transition from the dependence $\sigma \propto T^{1/2}$ to a stronger law occurs (Fig. 7, inset b). According to the existing theoretical conceptions, just such a change in the low-temperature behavior should be associated with a metal–insulator transition point.

Beginning at $T_{an} \geqslant 420$ K, the plot of $\rho(T)$ has an activation character (Fig. 6), the activation energy E_a increasing with T_{an} [Fig. 8(a)]. The asymptotic behavior $\rho \propto \exp(E_a/kT)$ is most clearly expressed for $T_{an} \geqslant 430-440$ K. We note that the metal–insulator transition point ($T_{an} \approx 420$) is associated with a thermopower feature [Fig. 8(a)]: for $T_{an} < 420$ K the Seebeck coefficient S lies in the range 2–10 μV/K and increases with T_{an}; at $T_{an}=420$ K the value of S decreases to 1 μV/K, and then for $T_{an} > 420$ K the thermopower increases sharply by more than three orders or magnitude, reaching values of $\sim 10^3$ μV/K, which are characteristic of semiconductors.

If we ignore the anomalous behavior of the thermopower and the data from the structural analysis presented in the preceding section, the picture of the metal–insulator transition in SiIII formally corresponds to a spatially homogeneous Fermi glass, the role of the "order parameter" being played by T_{an} (Figs. 7 and 8). It is obvious that the original sample is already fairly close to the mobility threshold, as is evinced by the low values of the Hall mobility and the existence of the asymptote $\sigma \propto T^{1/2}$. At the same time, it follows from Figs. 1, 4, and 5 that the experimental sample begins to be highly heterogeneous at $T_{an}=440$ K and apparently becomes a mixture of a metal (the remnants of SiIII) and a high-resistance insulator consisting of SiIV and disordered phases of silicon.

We note that the quasispatially homogeneous character of the metal–insulator transition first indicated, which fits the classical one-parameter scaling scheme[23,24] in the class of objects under consideration, was established for the case of the solid-phase amorphization of CdSb.[25] At the same time, on the basis of general arguments it seems very likely that the disordered insulating amorphous phase formed during solid-phase amorphization through a high-pressure phase appears on the boundaries of the metal grains and plays the role of insulating intervening layers, which distort and complicate the structure of the current lines.[26] In this case the metallic and insulating systems have the form of intermingled fractal regions, and the metal–insulator transition occurring during solid-phase amorphization must be a percolation, rather than a quantum, process.[26]

It was postulated in Ref. 11 for the class of metal–insulator transitions under consideration that both of these effects should be taken into account in the general case, i.e., a quantum metal–insulator transition takes place on a fractal object of reduced dimensionality during solid-phase amorphization. However, there is still no theory of metal–insulator transitions for this case that jointly takes into account the topological and quantum interference effects.

In the case of SiIII it is seen from the Raman and x-ray structural data that the ranges $T_{an} < 420$ K and $T_{an} > 450$ K correspond to two different phase states of the sample (Figs. 1–5). In the former case the sample is a polycrystal of SiIII containing no high-resistance phases of SiIV or a-Si, and in the latter case it is a mixture of microcrystalline SiIV and disordered silicon. We note that saturation of the $\rho(T)$, $S(T)$, and $E_a(T_{an})$ curves is observed in the latter case ($T_{an} > 450$ K) [Figs. 8(a) and 8(b)].

In the intermediate range $420 < T_{an} < 450$ K the sample is highly inhomogeneous and consists of a mixture of metallic (SiIII) and insulating regions (SiIV and disordered silicon phases).

Thus, in SiIII the metal–insulator transition takes place in a practically spatially homogeneous system ($T_{an} < 420$ K) and should be treated within a scaling scheme of quantum corrections (Fig. 7).

As is seen from the Raman data (Figs. 1–3), the increase in the degree of disorder in the system can be associated with relaxation of the stresses in the SiIII crystallites and with the resultant generation of structural defects. We note that variation of the deformation field can also induce variation of the density of states at the Fermi level for the semimetal SiIII, which, in turn, leads to variation of the thermopower $S(T_{an})$ (Fig. 8).

The percolation model can be more suitable in the range $420 \leqslant T_{an} \leqslant 450$ K. As follows from percolation theory, the changes in ρ and S in the vicinity of the percolation threshold coincide, and these quantities exhibit the same critical behavior.[27] It is seen from Fig. 8 that ρ and S measured at $T=300$ K have a similar functional dependence and increase

by three orders of magnitude in the range $T_{an}>420$ K. In such a system the role of the metal continues to be played by the lower resistance SiIII phase, which has greater conductivity than the disordered and microcrystalline silicon phases even in the insulating state (as follows from Fig. 8(b), the difference between the conductivities of SiIII at the metal–insulator transition point $T_{an}=420$ K and the insulating phases of silicon amounts to three to seven orders of magnitude).

At the same time, a purely percolation transition does not provide a satisfactory explanation for the strong increase in E_a with T_{an}. Therefore, remaining within this model, we should assume, in addition, that the characteristics of the insulating phases formed in the range $420<T_{an}<450$ K vary with the annealing temperature. Also, when the quantum regime is replaced by a percolation regime, a discontinuity or a jump would be expected on the plot of $\rho(T_{an})$, while the plot of $\rho(T_{an})$ is smooth over the entire range corresponding to the structural relaxation of SiIII [Fig. 8b].

Another interpretation of the observed picture of the metal–insulator transition in SiIII can be formulated on the basis of the microcrystalline structure of the sample.

It follows from the data from the structural analysis that the size of the crystallites is approximately equal to 20–30 Å and is somewhat greater than or of the order of the spatial scale of intermediate order, which assigns the size of the "troughs" or "crests" of a random potential in the amorphous phase. From the standpoint of the electronic properties, if the mean free path of the carriers exceeds this spatial scale, the sample can be regarded in all stages of the phase transformation as a single system, in which the random potential and/or the Fermi level vary in the annealing process. In such a system the picture of the metal–insulator transition will correspond to the analogous transition in a Fermi glass, as is observed experimentally (Figs. 6–8).

To conclude this section we note that the value of the conductivity of the system determined in the present work at $T=300$ K after completion of the phase transformations is consistent with the known published data.[2,6] According to Refs. 2 and 6, the magnitude of the band gap measured by optical methods amounts to about 0.65 eV in an annealed sample, and, therefore, the activation energy of ≈ 0.35 eV observed in our experiments for $T_{an}>450$ K is close to half of the band gap.

5. SEQUENCE OF PHASE TRANSFORMATIONS AND DISORDERING IN THE SiIII → SiIV STRUCTURAL TRANSITION

A comparison of the x-ray, optical, and galvanomagnetic experimental data reveals that the SiIII→SiIV phase transition takes place in several stages.

1. In the first stage ($T_{an}\leqslant 420$ K) the resistivity of the sample at $T=300$ K increases by more than two orders of magnitude while the quasimetallic character of $\rho(T)$ is maintained. However, neither the x-ray diffraction spectra nor the Raman spectra reveal the presence of an impurity of any crystalline modifications of silicon differing from the Kasper modification in the sample. At the same time, the Raman spectra contain additional maxima caused by stresses. Nevertheless, the intensity and width of the principal Raman maxima remain unchanged.

2. In the second stage of the transformation ($T_{an}=430$–450 K) the content of the Kasper phase decreases. For $T_{an}\approx 420$ K, the quasimetallic behavior of $\rho(T)$ is replaced by an activation dependence, and a metal–insulator transition takes place. For $T_{an}\geqslant 420$ K the activation energy increases smoothly until the resistivity stops changing ($T_{an}=480$ K) and then reaches saturation at a value of 0.35 eV. The total change in the electrical conductivity of the system in the region of the metal–insulator transition reaches a factor of 10^9.

In the Raman spectra the intensity of the principal Kasper Raman maxima decreases to zero, and a broad, poorly structured feature forms at 430–520 cm^{-1} for $T_{an}\geqslant 470$ K. The x-ray spectra of the sample in this stage of the transformation correspond to a mixture of microcrystalline and disordered phases: strongly broadened crystalline peaks of SiIV are superposed on the broad maxima.

3. In the third annealing stage ($T_{an}>480$ K) an appreciable quantity (20%) of diamond-like SiI forms in the sample, and its volume fraction increases with the temperature.

Thus, we have shown that considerable disordering of the sample occurs during the SiIII→SiIV structural transformation. This finding is of interest from the standpoint of the general problem of the relaxation of metastable high-pressure phases. However, although the data from the structural analysis and the results of the measurements of the galvanomagnetic effects obtained in the present work show that the sample is strongly disordered in the intermediate stage of the annealing, they do not admit an unequivocal conclusion regarding the formation of amorphous diamond-like *a*-Si. To further investigate the nature of the disordered state (*d*-Si) appearing when SiIII is annealed, we performed calorimetric measurements.

A heat-release curve obtained by scanning calorimetry with a heating rate of 20 K/min for a sample of SiIII is presented in Fig. 9. Besides the principal peak in the temperature range 450–530 K (Fig. 9, peak 1), there is also an extended, highly dispersed maximum (Fig. 9, peak 2) in the temperature range 550–630 K. The activation energy of the phase transformation calculated from the principal heat-release peak was 1.5 eV. The strong dispersion of the heat released in the second maximum precludes a reliable evaluation of the activation energy of the corresponding process. Because the heat-release curve was measured at a finite heating rate, the heat-release peaks are shifted toward higher temperatures in comparison with those obtained under isothermal conditions. When this is taken into account, the first peak corresponds to the relaxation of SiIII with a heat $\approx$ 8 kJ/mole. The second maximum could be associated with the crystallization of "amorphous" silicon (we recall that an increase in the amplitude of the crystalline lines is observed in this temperature range according to the data from the structural analysis). However, the heat measured for this maximum amounts to approximately 0.5 kJ/mole, while the heat of crystallization for *a*-Si exceeds 12 kJ/mole (Ref. 28).

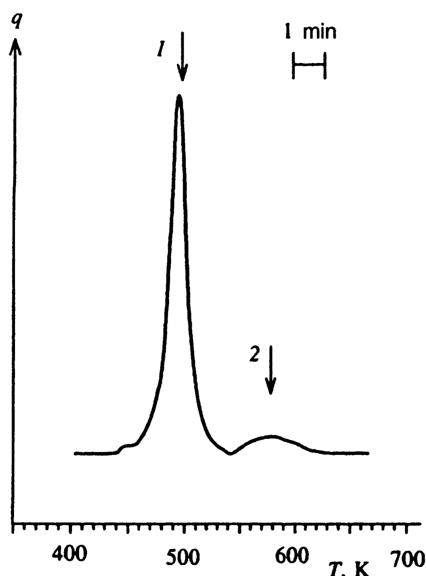

FIG. 9. Heat-release curve during the annealing of SiIII.

This discrepancy can be explained in several ways. First, the samples investigated are finely dispersed and, therefore, contain a considerable number of phase boundaries. In this case the crystallization process is associated with alteration of the structure and energy of the phase boundaries, and, as a result, the total heat released can be smaller than in the case of spatially homogeneous a-Si films.

Second, the lonsdaleite modification SiIV, rather than the diamond-like modification, forms when SiIII relaxes. Therefore, it is natural to assume that the short-range order in the disordered phase, d-Si, will correspond to SiIV, rather than SiI, and consequently a value of the heat differing from that for the crystallization of a-Si can be expected.

Interestingly, the appearance of the disordered state of d-Si can be explained qualitatively within the crystal-geometric model of the SiIII→SiIV phase transition.[29,30] According to this model, the atoms found in planes 1, 4, 6, and 9 of the Kasper unit cell (see Fig. 10) move in these planes without departing from them during the transformation, and the set of planes experiences extension along the normal axis amounting to 5.8%. The atoms in these planes subsequently form the centers and bases of the tetrahedrons of the lonsdaleite phase. Cleavage of the bonds lying in the plane of a layer followed by the formation of new interlayer bonds also takes place. One member of the family of equivalent directions of the SiIII phase, viz. [100], becomes the z axis of the hexagonal cell of the lonsdaleite phase.

The lowering of the crystallographic symmetry in the SiIII→SiIV transition is very important. In the isotropic cubic cell any of the equivalent directions [100], [010], or [001] can become the z axis of the hexagonal cell. If the dynamic correlation in the cleavage of the bonds extends over a length of moderate order (i.e., over a distance of four to five atomic layers), the degeneracy with respect to the direction of the z axis of the hexagonal system can cause the cleavage of bonds lying in mutually perpendicular layers to occur even on scales of order the size of the cell of the Kasper phase (5–15 Å) and, therefore, a cell of considerable size with well defined hexagonal point symmetry does not form. This factor can promote the appearance of a highly disordered phase with a configuration of covalent bonds close to SiIV. This possibility is facilitated by the appreciable increase in the specific volume ($\approx 8\%$) in the SiIII→SiIV transition and the resultant appearance of local stresses in the volume of the sample.

Thus, the set of data obtained in the present work, including the data on the metal–insulator transition, allows us to postulate that the Kasper phase of silicon apparently relaxes according to the scheme

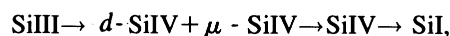

$$\mathrm{SiIII} \rightarrow d\text{-}\mathrm{SiIV} + \mu\text{-}\mathrm{SiIV} \rightarrow \mathrm{SiIV} \rightarrow \mathrm{SiI},$$

where d-Si and μ-SiIV are, respectively, disordered and microcrystalline phases based on the lonsdaleite modification of silicon. The testing of this hypothesis is a task for future studies.

This work was performed with financial support from the Russian Foundation for Fundamental Research (Grants Nos. 95-02-03815a and 05-02-03677), the International Science Foundation (Grant No. MTK300), and the "Fullerenes and Atomic Clusters" Russian National Program. Several phases of this study were performed as part of joint projects of the Royal Society (Great Britain) and INTAS (INTAS Projects 93-2400, 94-1788, and 94-4435).

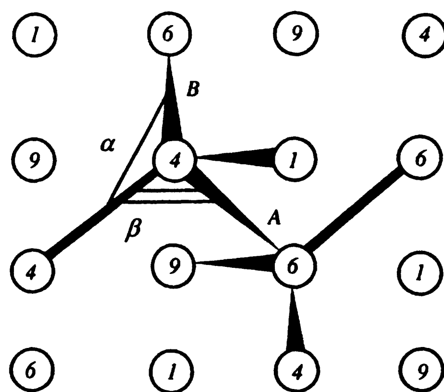

FIG. 10. Diagram of the short-range order in the Kasper phase of silicon (see explanations in the text).

[1] J. Kasper and R. Wentorf, Acta Crystallogr. **17**, 752 (1964).
[2] G. Weill, J. L. Mansot, G. Sagon, and J. M. Besson, Semicond. Sci. Technol. **4**, 280 (1989).
[3] R. Kobliska, S. Solin, M. Selder, *et al.*, Phys. Rev. Lett. **29**, 725 (1972).
[4] M. Hanfland and K. Syassen, High Press. Res. **3**, 242 (1990).
[5] J. Kasper and R. Wentorf, Science **139**, 338 (1963).
[6] J. M. Besson, E. H. Mokhtari, J. Gonzales, and G. Weill, Phys. Rev. Lett. **59**, 473 (1987).
[7] R. Biswas, R. M. Martin, R. J. Needs, and O. H. Nielsen, Phys. Rev. B **35**, 9559 (1987).
[8] M. T. Yin, Phys. Rev. B **30**, 1773 (1984).
[9] J. Joannopulos and M. Cohen, Phys. Rev. B **7**, 2644 (1973).
[10] M. Yin and M. Cohen, Phys. Rev. Lett. **45**, 1004 (1980).
[11] S. V. Demishev, Yu. V. Kosichkin, N. E. Sluchanko, A. G. Lyapin, Usp. Fiz. Nauk **164**, 195 (1994) [Phys. Usp. **37**, 185 (1994)].
[12] E. G. Ponyatovsky and O. I. Barkalov, Mater. Sci. Rep. **8**, 147 (1992).
[13] S. V. Demishev, T. V. Ishenko, and F. V. Pirogov, Fiz. Tverd. Tela (St. Petersburg) **37**, 608 (1995) [Phys. Solid State **37**, 331 (1995)].
[14] S. V. Demishev, Yu. V. Kosichkin, D. G. Lunts, *et al.*, Zh. Éksp. Teor.

Fiz. **100**, 707 (1991) [Sov. Phys. JETP **73**, 394 (1991)].
[15] S. V. Demishev, Yu. V. Kosichkin, A. G. Lyalin, *et al.*, Zh. Éksp. Teor. Fiz. **104**, 2388 (1993) [JETP **77**, 68 (1993)].
[16] L. G. Khvostantsev, L. F. Vereshchagin, and A. P. Novikov, High Temp. High Pressures **9**, 637 (1977).
[17] R. Kobliska and S. Solin, Phys. Rev. B **8**, 3799 (1973).
[18] J. M. Perez, J. Villalobos, P. McNeill, *et al.*, Appl. Phys. Lett. **61**, 563 (1992).
[19] E. Bustarret, M. A. Hachicha, and M. Brunel, Appl. Phys. Lett. **52**, 1675 (1988).
[20] *Light Scattering in Solids I (Topics in Applied Physics, Vol. 8)*, edited by M. Cardona (Springer, Berlin, 1975) [Russ. transl., Mir, Moscow, 1979].
[21] M. Richter, Z. Wang, and Z. Ley, Solid State Commun. **39**, 625 (1981).
[22] V. I. Iveronova and G. P. Reakevich, *Theory of the Scattering of X-Rays* [in Russian] (Izd. MGU, Moscow, 1978), p. 129.
[23] I. P. Zvyagin, *Kinetic Phenomena in Disordered Semiconductors* [in Russian] (Izd. MGU, Moscow, 1984).
[24] N. B. Brandt, S. V. Demishev, A. A. Dmitriev, *et al.*, Zh. Éksp. Teor. Fiz. **86**, 1446 (1984) [Sov. Phys. JETP **59**, 847 (1984)].
[25] V. M. Teplinskiĭ, V. F. Gantmakher, and O. I. Barkalov, Zh. Éksp. Teor. Fiz. **101**, 1698 (1992) [Sov. Phys. JETP **74**, 905 (1992)].
[26] V. M. Teplinskiĭ, V. F. Gantmakher, and S. É. Esipov, Zh. Éksp. Teor. Fiz. **97**, 373 (1990) [Sov. Phys. JETP **70**, 211 (1990)].
[27] V. V. Brazhkin, S. V. Demishev, Yu. V. Kosichkin, *et al.*, Zh. Éksp. Teor. Fiz. **101**, 1908 (1992) [Sov. Phys. JETP **74**, 1020 (1992)].
[28] W. C. Sinke and S. Roorda, J. Cryst. Growth **69**, 222 (1990).
[29] V. D. Blank and Z. V. Malyushitskaya, Kristallografiya **37**, 724 (1992) [Sov. Phys. Crystallogr. **37**, 382 (1992)].
[30] V. D. Blank and Z. V. Malyushitskaya, Kristallografiya **38**, 179 (1993) [Crystallogr. Rep. **38**, 229 (1993)].

Translated by P. Shelnitz